Soft Matter

Accepted Manuscript

ROYAL SOCIETY OF CHEMISTRY

www.rsc.org/softmatter

TOC : A colloid-probe AFM based approach investigates the interaction between protein coatings on colloid probes and surface decorated with close-packed colloidal crystal layer.

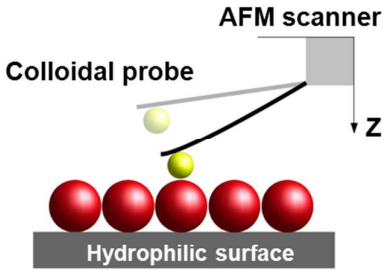

Cite this: DOI: 10.1039/c0xx00000x

www.rsc.org/xxxxxx

ARTICLE TYPE

Colloid-probe AFM studies of the interaction forces of proteins adsorbed on colloidal crystals

Gurvinder Singh,[ab] Kristen E. Bremmell,[c] Hans J. Griesser,[d] and Peter Kingshott*[ae]

Received (in XXX, XXX) Xth XXXXXXXXX 20XX, Accepted Xth XXXXXXXXX 20XX

DOI: 10.1039/b000000x

In recent years, colloid-probe AFM has been used to measure the direct interaction forces between colloidal particles of different size or surface functionalities in aqueous media, as one can study different forces in symmerical systems (i.e., sphere-sphere geometry). The present study investigates the interaction between protein coatings on colloid probes and hydrophilic surfaces decorated with hexagonally close packed single particle layers that are either uncoated or coated with proteins. Controlled solvent evaporation from aqueous suspensions of colloidal particles (coated with or without lysozyme and albumin) produces single layers of close-packed colloidal crystals over large areas on a solid support. The measurements have been carried out in an aqueous medium at different salt concentrations and pH values. The results show changes in the interaction forces as the surface charge of the unmodified or modifed particles, and ionic strength or pH of the solution is altered. At high ionic strength or pH, electrostatic interactions are screened, and a strong repulsive force at short separation below 5 nm dominates, suggesting structural changes in the absorbed protein layer on the particle. We also study the force of adhesion, which decreases with an increment in the salt concentration, and the interaction between two different proteins indicating a repulsive interaction on approach and adhesion on retraction.

1. Introduction

Protein adsorption to solid supports has remained under intense investigation for several decades as it is of crucial importance in many practical applications including medical device coatings, drug delivery, and food processing.[1-3] From a medical perspective, uncontrolled deposition of proteins on an implant surface causes adverse biological responses, and blockage of filtration membranes in bio-separation processes.[4, 5] In a favourable way, protein adsorption is utilized for food colloid stabilization,[6] and the development of biosensors and biochips.[7, 8] With the continous progress in nanomaterials synthesis, new types of hybrid biomaterials incorporating protein/enzymes on colloidal nanoparticles has been increasingly used in several biomedical applications.[9] The protein can either bind to particles physically or be chemically immobilised, and their surface characteristics can be controlled by tuning the surface chemistry, sizes and geometry of the surface.[10-13]

Moreover, curved surfaces, which are always preferred over flat surfaces for protein adsorption, allow ultrasenstive detection.[7, 14] Therefore, understanding protein-protein and protein-surface interactions is essential and requires accurate measurement of interaction forces at the nanoscale. Colloidal particles are a suitable model system to investigate these fundamental interactions since the interaction forces between many colloidal particles can be well described by Derjaguin, Landau, Verwey and Overbeek (DLVO) theory incorporating contributions from electrostatic and van der Waals forces.[15]

Several techniques have been developed for the direct measurement of forces between two surfaces.[16-18] Recently, McNamee et al. has designed a Monolayer Particle Interaction Apparatus to directly measure forces between a monolayer at an air/water interface and a particle in solution.[19] However, atomic force microscopy (AFM) has emerged as a more powerful technique since it isdemonstrated to have an ability to acquire fast force measurements. A suitable approach for the detection and theoretical modelling of small forces with high sensitivity is the so-called colloid-probe AFM technique in which a colloidal sphere is attached to the AFM cantilever. It was first introduced by Ducker et. al. and Butt et. al., where they used silica and glass spheres respectively for their force measurements.[20, 21] Colloid-probe-AFM is based on measuring the deflection of a very sensitive cantilever, while it is approaching or being retracted from a surface. The measured cantilever deflection is transformed into force data by using the spring constant of the cantilever, and is displayed as a function of the probe surface separation distance.

Numerous investigations have been reported to measure forces for unsymmertic systems, i.e., the interaction between a planar surface and particle (colloid-probe). For example, this system has been widely used for understanding protein-protein

interactions,[22-25] and protein interactions with different materials under physiological conditions.[26-28] In addition, it has also been used for studying bare surface-surface interactions,[29-31] and bacterial interactions to different surfaces in aqueous conditions.[32] Cell morphology, defective cell detection and its mechanical properties have also been investigated using colloid-probe AFM.[33, 34] Only a few reports exist on the interaction between symmetric systems, i.e., sphere-sphere geometries.[35, 36] In recent years, Borkovec et al. have introduced a novel variant of this technique, termed as multiparticle colloid-probe AFM providing a large surface area of interaction. They have studied the interaction between charged particles of a few µm in size in the presence of various type of polyelectrolytes.[37, 38] Such measurements require lateral alignment of two particles centerally which can be obtained by first scanning a region of interest.

Herein, we present a modified multiparticle colloid-probe AFM based approach to investigate the interaction between a colloid-probe and close packed arrays of micron sized colloidal particles self-assembled onto a surface. Prior to assembly, the colloidal particles were modified with different types of proteins. Previously, we have successfully shown that protein coated particles can self-assemble in hexagonal close-packed arrays over centimeter sized areas.[39] We follow a similar approach to form self-assembled particle layers and study the interaction between proteins adsorbed on the particle surface and their interaction with various materials under different salt concentration solutions. For this work, polystyrene and silica colloidal particles were chosen as a model system as they are easily available with a range of functionalities, allowing adsorption of biomolecules such as proteins, antibodies, etc. Globular proteins of opposite surface charge, lysozyme and bovine serum albumin were selected for this study not only as they are model proteins (Table 1), but they are also key adsorbates on implant surfaces exposed to biological fluids.

Protein	Mass (Da)	Size (nm)	pI (iso-electric point)
Lysozyme (LZM)	14000	4.0 x 3.0 x 3.0	11.1
Bovine Serum albumin (BSA)	66000	14.0 x 4.0 x 4.0	4.7

Table 1 Properties of the proteins[40, 41]

2. Experimental

2.1 Materials

Mono-disperse 2 µm carboxyl (COOH) polystyrene (PS) particles (4 wt%) were purchased from Invitrogen (USA). Mono-disperse 2 µm plain silica particles (9.8 wt%) were bought from Polysciences Europe GmbH (Germany). These particles were stored at 4°C. Absolute ethanol (Sigma Aldrich, HLPC grade), toluene (Sigma Aldrich, ≥99.5%), polyethylenimine (PEI) (Molecular weight 25,000) and sodium chloride (NaCl) were used as received. Lysozyme (LZM) from chicken egg white (lyophilized powder) and albumin from bovine serum (BSA) (lyophilized powder) were purchased from Sigma Aldrich. Boron doped silicon wafers with a diameter of 76.2 mm, orientation (100) and a resistivity of 0.0005–0.001 Ω cm were obtained from Virginia Semiconductors (Virginia, USA).

2.2 Protein Adsorption and Assembly Formation

Prior to use, the particles were brought to room temperature by sonicated for 30 min. A few µl of particles were dispersed in freshly prepared protein solution (1 mg/mL) in PBS buffer (pH=7.4) for a duration of 2 hours at room temperature. After protein adsorption, particle suspensions were washed three times with PBS buffer, and once with Milli-Q water using a centrifuge, and particles were re-dispersed in Milli-Q water. NaCl solutions of different concentration were prepared in Milli-Q water. Silicon wafers cut into 1 cm^2 pieces were cleaned by 15 min sonication each in solutions of ethanol, toluene and ethanol, followed by drying with N_2 gas. The cleaned substrates were then UV-ozone treated to achieve a more hydrophilic surface. The approximate concentration of the particles (V_P in µl) confined in the ring of a particular diameter (D_R in cm) can be calculated by the following derived formula

$$V_P = \frac{10\times\pi\times\rho\times D_P\times D_R^{"}}{12\times w} \quad (1)$$

Where ρ is the density of particles (g/cm^3), D_P is the diameter of the particle (µm), and w is the % solid content of the particle suspension. The calculated amount of the particles is enough to make a one layer of particles, and number of colloidal layers can be built up by increasing the concentration of particles. For example, to make one layer of 2 µm COOH-PS colloidal crystals inside a 1 cm diameter rubber ring, 1.8 µL of 2 µm particles were mixed in 100 µL Milli-Q water (0.5 µS/cm conductivity). The prepared colloidal suspension was left for 30 minutes to allow them to be well dispersed. Rubber rings were cleaned thoroughly by sonication in ethanol and Milli-Q water each for 15 min. After fixing the rubber ring to the substrate, the colloidal suspension was pipetted carefully inside the ring. The substrate was then kept in a vacuum desiccator at room temperature until complete evaporation of the solvent was achieved, which typically took 2-3 hours, depending upon ambient temperature and humidity. The colloidal particles were modified with PEI (1 mg/mL) at room temperature for 1 hour, followed by successive washing three times in Milli-Q water using a centrifuge. The PEI modified particles were again dispersed in Milli-Q water and stored at 4°C.

2.2 Force Curve Measurements

All force curves were acquired with a Nanoscope III AFM (Digital Instrument, USA) using the colloid-probe technique in a

commercial fluid cell. Colloid-probes of 1 μm plain PS were purchased from Novascan Technologies (Ames, IA, USA) and used after careful cleaning in ethanol and water. The probe was cleaned every time before use. The spring constant of the cantilevers was determined by the method of thermal tuning and found to be 0.032±0.013 N/m.[42] Colloid-probes were coated with albumin (1 mg/ml solution in PBS buffer) by dipping in a drop of solution for 2 hours, followed by rinsing three times in PBS buffer and Milli-Q water carefully. It should be noted that self-assembled monolayers from particles with or without protein, as well as protein modified AFM probes were dried prior to force measurements in aqueous environment. The force curves were measured after a conditioning period of 15 min for each solution. First, we scanned the samples by fluid contact mode AFM using the 1 μm PS probe over 15 μm^2 area, and then, the magnified area of ~2.5 μm^2 around a single particle was scanned. Assuming the probe cantered over the single particles with precision of ~100 nm, the force curves were collected. The raw data were exported into an Excel spreadsheet and converted into normalized force ($F/2\pi R_f$) versus apparent separation, where R_f is the effective radius. The surface potential (i.e., Zeta potential, ζ) of all particles was measured using a Zetasizer Nano series (Malvern instrument, UK). We have assumed the surface potential of the colloid-probe to equal that of the 1 μm colloid particles of the same chemistry for the analysis of force curves.

3. Theory

According to DLVO theory, the total interaction force between two spherical particles is given by

$$F = F_{EDL} + F_{vdW} \quad (2)$$

where F_{EDL} is the electrical double layer (EDL) force and F_{vdW} is the attractive London van der Waal force. This is a convenient approach for illustrating interactions between colloidal particles in aqueous solution, but this theory does not incorporate other forces such as hydration, steric, etc. The electrical double-layer force (F_{EDL}) can be obtained by solving the Poisson-Boltzmann (PB) equation in linear or non-linear approximations. The solutions of these approximations were solved elsewhere in the literature.[43, 44] The program that we employed for analysis uses the linear Poisson-Boltzmann equation for rigid bodies at large separations to set up the zero of experimental separation. This method is also applicable to soft bodies if they behave as rigid bodies for weak forces and require the determination of surface potential independently. The linear PB equation for the electrostatic interaction between the two spheres is

$$F_{EDL} = 4\pi\varepsilon\varepsilon_o R_f \kappa \gamma_1 \gamma_2 \left(\frac{4k_BT}{q}\right)^2 e^{-\kappa d} \quad (3)$$

Where ε_o is the permittivity of free space, ε the permittivity of aqueous medium, R_f is effective radius

$$R_f = \frac{R_1 R_2}{R_1 + R_2} \quad (4)$$

k_B is Boltzmann's constant, T is the absolute temperature, q is the ionic charge, d is the separation, and κ^{-1} is the Debye length measuring the thickness of EDL,

$$\kappa = \sqrt[2]{\frac{e^2 \sum_i z_i^2 n_i}{\varepsilon\varepsilon_o k_B T}} \quad (5)$$

Here, z_i are the ion valences, and n_i is the ion concentrations. The renormalized surface potential is given by

$$\gamma = \tanh\left(\frac{q\varphi}{4k_BT}\right) \quad (6)$$

where φ is the surface potential.

Results for the attractive London-van der Waals force are obtained for a variety of geometries. For the first-order approximation,

$$F_{vdW} = \frac{AR_f}{6d^2} \quad (7)$$

where A is the Hamaker constant. Therefore, the net interaction acting between two spherical particles can be written as

$$\frac{F}{2\pi R_f} = 2\pi\varepsilon\varepsilon_o \kappa \gamma_1 \gamma_2 \left(\frac{4k_BT}{q}\right)^2 e^{-\kappa d} + \frac{A}{6d^2} \quad (8)$$

4. Results and Discussion

Fig. 1a is a schematic of self-assembled colloidal particle layer formation. The aqueous suspension of colloidal particles spreads over the surface encircled by the O-ring, and subsequently, complete evaporation results in a single self-assembled close-packed colloidal crystal layer. The detailed mechanism of its formation is described elsewhere,[45, 46] but briefly, it comprises mainly electrostatic, capillary, and convective flow forces to induce crystallization of the colloids. A typical AFM height image of the 2 μm COOH-PS particle monolayer taken from a 1 μm colloid-probe is displayed in Fig. 1b indicating the close-packed arrangement of particles is a hexagonal array. The cross-section analysis of the AFM image shows particle separation (center to center distance) of ~2 μm. Later, force curves were measured over several individual particles by colloid-probe and normalized to the effective radius of both particles.

We first discuss the interaction between the colloidal particles bearing no adsorbed proteins. The representative approach force curve profiles between the colloid-probe and solid supported 2 μm COOH-PS particles are shown in Fig 2a. The interaction at large separation is repulsive in nature, since both surfaces bear negative potentials at an ionic strength of 1 mM NaCl solution (Table 2). To confirm the origin of the interaction, DLVO theory was used to fit the force curve profiles of colloid-probe/COOH-PS system (Equation 8). The surface potentials of the particles were directly obtained from ζ-potential measurements to solve the P-B equation (Equation 3). As a result, the DLVO theory fitted well the experimental force curve at large separations indicating the repulsive EDL interaction originating from the overlap of the diffuse layers.[37, 38] Similar interactions were also observed between the PS colloid-probe and 2 μm silica particles (Fig. 2b).

To examine the effect of particle surface charge on the interaction, the surface charge of the 2 μm COOH-PS particles was reversed by a physically adsorbed layer of PEI. Their measured zeta potentials were approximately the same in magnitude but of opposite sign ($\varphi_{probe\text{-}PS}$= -28.9 mV and $\varphi_{2\mu m\text{-}PS(PEI)}$= +29.4 mV). An electrostatic repulsive interaction acting between the surfaces was not observed, instead a rather small attractive interaction appeared at large separation leading to an attractive van der Waals force below 10 nm (Fig. 2c). After fitting the force curve with the DLVO model using measured zeta potentials, the attractive interaction was found to be less than that predicted by the theory. The best fit shown in Fig. 2c corresponds to a surface potential of +5.0 mV which is substantially smaller than +29.4 mV measured by the zeta-sizer. A similar disagreement was observed for the interaction between the sulfate latex in the presence of PEI and explained in the terms of heterogenous adsorption.[38] We also suspect that this decrease in surface potential may arise from potential adsorption of some carbonaceous materials from atmosphere on the dried crystal layer of particles before measuring the force curve profiles.

Let us now discuss the interaction between a bare colloid-probe and a LZM modified 2 μm COOH-PS particle patterned surface at 1 mM NaCl, as depicted in Fig. 3a. This force profile is similar to one obtained as shown in Fig. 2a, however, a smaller range of electrostatic repulsion was noticed when 2 μm particles were coated with LZM. LZM is assumed to have an overall positive charge regulating the surface charge of the negatively charged COOH-PS particles after adsorption from PBS buffer (pH=7.4). A decrease in ζ-potential further confirms the LZM adsorption on negatively charged particles indicating a slightly negative potential (-4.7 mV) in 1 mM NaCl. These observations are in good agreement with previous studies of LZM adsorption at a charged interface.[47, 48] The change in surface potential from more negative to less negative or slightly positive is interpreted as either a change in pH at the interface or adsorption induced neutralization of the surface potential.[48] Therefore, the colloid-probe experiences a rather weak repulisve force against LZM coated particles, which onsets at a separation of approximately 20-25 nm in comparison to protein uncoated COOH-PS particles (~35-40 nm). In addition, the force curve fitting using zeta potentials ($\varphi_{probe\text{-}PS}$= -28.9 mV, and $\varphi_{2\mu m\text{-}PS(LZM)}$= -4.7 mV) shows a close agreement with DLVO theory at a large separation. Similar behaviour of force curve profiles was also observed in case of PS colloid-probe and LZM coated 2 μm silica particles (Fig. 3b).

The influence of ionic strength (IS) on the interaction between the PS colloid-probe and LZM modified 2 μm COOH-PS particle patterned surface was also studied. The force curve profiles indicate a decrease in the electrostatic repulsive interaction with increasing IS from 1 mM to 100 mM NaCl (Fig. 4a). The increase in IS of the solution screens the electrostatic interactions and reduces their range of interaction in such a way that at 100 mM NaCl and above this concentration, these electrostatic repulsive forces are negligible. A similar trend of force curve profiles with increasing IS has also been observed in the case of the colloid-probe and LZM-coated 2 μm silica particle patterned surface where the force curve in 1 M NaCl represents two regimes; above and below a separation distance of 4 nm approximately (Fig. 4b). At distances greater than 4 nm, there is practically no repulsive interaction as salt ions screen the charges on both surfaces (i.e., LZM coated particle and colloid-probe). An attraction onsets at a separation distance of approximately 7 nm before the colloid-probe touches the protein at a distance of approximately 4 nm. This attraction is due to van der Waals dispersion interactions which usually dominate in this range (i.e., below 10 nm). These results are in full accord with previous studies measuring the force curve profiles between a colloid-probe and BSA layer adsorbed on a flat silica surface.[23] LZM is a globular protein, and highly ordered in its native state in aqueous solution. The effective size of an adsorbed protein depends on Debye length (κ^{-1}) and the charge density on the exposed protein surface which can be tuned by varying the salt concentration and pH of the solution.[49, 50] When an adsorbed protein layer is exposed to an increasing ionic strength solution, the electrostatic repulsive forces between the protein molecules within adsorbed layer or between the protein and surface diminish, and intra-molecular forces between the protein molecules dominate.[23, 51-53] Thus, the adsorbed layer becomes more compact and rigid than at lower IS. If we assume this effect, the compactness and rigidity of adsorbed layers can also be inferred from contact regions in the force curve profiles in Fig. 4a and 4b. The slope of the compliance region of the AFM approach curves (i.e., zero distance regime) provide evidence for elastic properties of the adsorbed protein layer (i.e., the slope represents the amount that colloid-probe can be compressed into the polymer layer).[54] In our case, the slope of the approach curve increases as the IS of the solution increases, indicating the more compact and rigid the adsorbed layer is at high IS compare to a more compliant layer at low IS. This observation implies that at higher IS, where electrostatic repulsions are screened, LZM acquires a compact structure.[51, 55] A similar effect was also reported for different proteins by Tsapikouni et al. and Zhang et al.[28, 56]

Fig. 4c shows the force profiles between LZM-coated 2 μm silica and colloid-probe at different pH values of 4, 7.4 and 11.1. In this set of experiments, the IS was kept constant at 1 mM NaCl. At pH values below 11.1, a colloid probe experiences less electrostatic repulsive interactions against LZM-coated particles during approach below 10 nm, and the maximum repulsive forces were measured at a shorter separation distance of 5 nm. As the pH of the aqueous solution is increased to 11.1 (iso-electric point of LZM protein), the repulsive force weakens, and a short range attractive force sets in at ~7 nm before contact to the surface. In this case, a maximum repulsion (hard wall interaction) was measured approximately at a short separation of 2.5 nm. In addition, the slope of the contact region is greater than the slope measured at other pH values. Dependence of the force curve at this pH is analogous to the force profile at high IS (i.e, 100 mM) pointing to a compact absorbed layer of LZM. These findings are consistent with previous reports where pH-induced conformational changes in various proteins have been investigated by different techniques including colloid-probe AFM, neutron reflectivity, and surface force appartus.[23, 56-58] Moreover, plausible models have been proposed to explain the

pH dependence of the thermodynamic stability of proteins.[59, 60] The stability of protein molecules is determined by electrostatic interactions in the native, folded state of a protein. At the extremes of acidic or basic pH values, the decreased stability may result in unfavorable electrostatic interactions introduced by an increase in positive or negative charge on a protein. The theory predicts maximum stability (i.e., a compact structure) at or near the isoelectric point of the protein where the net charge is zero.[59, 60]

In this work, the forces upon retraction, e.g., the force of adhesion were also analyzed. The retraction force profile curves between a bare colloid-probe with or without LZM adsorbed on 2 µm COOH-PS particles at 1 mM NaCl are illustrated in Fig. 5a. It is seen that the adhesive force for a 2 µm COOH-PS particle patterned surface is larger than that for LZM coated 2 µm COOH-PS particle array. When a probe is pressed into contact with the surface with sufficient force, the molecules present at surfaces will rearrange, bridge and then bind both surfaces until a high enough force is reached to detach a probe from the surface.[54] The force of adhesion depends on the number of binding sites between the two surfaces, and requires a large force in comparison to the force to bring two surfaces close to each other. Here, a colloid probe feels less interaction (i.e., forming fewer number of bonds) towards LZM coated particle array indicating week adhesion. While comparing approach curves of Fig. 2a and 3a, the extent of large electrostatic repulsion between the probe and COOH-PS particles can be inferred compared with that for the probe and LZM coated COOH-PS particles further confirming the large adhesion of a probe against COOH-PS particles. Although, these particles bear hydrophilic functional moieties on their surface such as carboxyl groups, the particles remain hydrophobic due to their high contact angle >90°. Therefore, the appearance of adhesive forces can be attributed to the short range hydrophobic forces. Furthermore, these hydrophobic forces can also be responsible for adhesive interaction between probe and LZM coated particles due to the presence of hydrophobic patches on the protein.[63]

An effect of IS on the retraction force profiles between a colloid-probe and LZM coated 2 µm COOH-PS particle array is shown in Fig. 5b. An increment in salt concentration results in a decrease in the magnitude of force of adhesion. The change in the force of adhesion with increasing IS can be understood assuming occupancy of the number of binding sites of LZM residues with salt ions which may screen their ability to take part in the interaction.[64] In high salt concentration, many of the binding sites are bound with salt ions, resulting in a weaker adhesive force against the probe than to the forces experienced in low salt concentration.[52, 56] Moreover, the results from retraction force curve profiles at different IS are in good agreement with approach force curve profiles as seen in Fig. 4a confirming the compact and rigid layer of absorbed protein which provides fewer number of binding sites to the colloid-probe resulting a weak force of adhesion at high IS. This observation is in accord with previous investigations for the same or different protein systems.[24, 28, 53, 56]

To elucidate protein-protein interactions, herein, the interaction between the LZM and BSA proteins adsorbed onto a solid curved support were also investigated. The results of the force measurements between a BSA coated PS colloid-probe and a LZM coated 2 µm COOH-PS (LZM) array at a salt concentration of 1 mM NaCl are presented in Fig.6. The net interaction on approach between the BSA modifed PS probe and LZM coated 2 µm particle patterned surface is repulsive reaching to maxium at a separation below 5 nm. When the experimentally measured normalized approach force curve is compared to DLVO theory (solid line) using potentials ($\varphi_{probe\text{-}PS(BSA)}$= -13.9 mV and $\varphi_{2\mu m\text{-}PS(LZM)}$= -4.7 mV), no fit was seen at all separations. In these experimental conditions, an additional contribution arising from steric repulsion to DLVO theory may improve the fit.[23] Observation of a repulsive force when the BSA is negatively charged (pH > p*I*) and the LZM positvely charged (pH < p*I*) was unexpected. However it was consistent with our previous investigation, where there was no evidence of aggregation when BSA and LZM coated PS particles were mixed in aqueous solution phase, indicating a stable solution of mixed BSA and LZM protein coated particles.[39] Interaction forces on retraction showed different traces, Fig. 6b displays the most representative retraction force curve profile for each system. It should be noted that we did not observe any plateaus in retraction force profiles, however, a range in maximum adhesion was noticed for both systems. On an average, a large force of adhesion between BSA modified probe and LZM coated particle (0.14±0.04 nN) in comparison to adhesion between a bare probe and LZM modified particle (0.04± 0.03 nN) was observed which can be attributed to a larger extent of entanglements or interaction between the two protein molecules when both are compressed against each other. On pulling off the probe from the surface, breaking of different contact points between the protein molecules appear until the probe is completely pulled up from the particle surface.[24, 37, 65]

Finally, we cannot ignore the possibility of denaturing of protein molecules as it is difficult to note the extent of conformation change by looking into difference in force curve. However, based on a previous investigation,[39] there are less chances of protein denature upon drying and subsequent wetting where specific binding of antibody to lysozyme coated particles was demonstrated. Furthermore, a recent ToF-SIMS study of Filgrastim (a globular protein) demonstrated a difference in conformation between an adsorbed protein molecule and an adsorbed partly denatured protein molecule, suggesting that drying the adsorbed proteins under high vacuum did not lead to significant denaturation.[66]

5. Conclusion

Colloid-probe AFM has been employed to measure the forces of interaction between colloidal particles of different size. Ordered patterned surfaces of 2 µm particles were fabricated by an evaporation induced method on which a colloid-probe (bare or modifed with protein) examines the interactions with the individual particles. A bare probe experiences changes in force varying from repulsive to less repulsive or attractive depending on the net surface charge of the unmodified or modified particles. DLVO theory was used to fit these experimental curves with the help of the P-B equation using surface potentials as a fitting

parameter, and their fits were found to be satisfactory. The results indicate that the range of repulsive interactions can be tuned by varying a ionic strength and pH of the solution. In high IS and pH solution, the probe feels a very strong replusion at very short separation indicating some changes in absorbed protein layer (i.e., more rigid layer). Similarly, the strength of adhesive force decreases with increases in IS. These changes in the absorbed layer of protein may be associated with conformational changes in LZM. The colloid-probe AFM provided a qualitative analysis to understand changes in absorbed protein layers under different aqueous conditions. The results also show that two different proteins (i.e., interaction of BSA with LZM) absorbed on particles result in a strong repulsion on approach while multiple point breaking in the retraction force curve occurs. Thus, understanding of the cause-and-effect relationship governing these protein-particle or protein-protein interactions has the potential to lead to design of adsorbed-biomolecule systems with improved performance for a broad range of applications in biomedical engineering and biotechnology. In future perspective, the approach developed in this study can be applicable to a wide variety of biomolecule surfaces to investigate qualitatively how different aqueous conditions influence conformation or adsorbed-state properties of proteins at the molecular level.

Acknowledgements

This work was funded through a Danish Research Council Internationalisation PhD Stipend and the Ian Wark Research Institute, University of South Australia.

Notes and references

[a] *Interdisciplinary Nanoscience Centre, Faculty of Science, Aarhus University, Ny Munkegade, Aarhus C 8000, Denmark*
[b] *Department of Materials Science and Engineering, Norwegian University of Science and Technology, N-7491 Trondheim, Norway*
[c] *School of Pharmacy and Medical Sciences, University of South Australia, Adelaide 5000, Australia*
[d] *Mawson Institute and Ian Wark Research Institute, University of South Australia, Mawson Lakes, SA 5095, Australia*
e Industrial Research Institute Swinburne (IRIS) and Department of Chemistry and Biotechnology, Faculty of Science, Engineering and Technology, Swinburne University of Technology, Hawthorn, 3122 VIC, Australia. E-mail: pkingshott@swin.edu.au

1. T. J. Webster, L. S. Schadler, R. W. Siegel and R. Bizios, *Tissue Eng*, 2001, **7**, 291-301.
2. I. Brigger, C. Dubernet and P. Couvreur, *Adv Drug Deliver Rev*, 2002, **54**, 631-651.
3. D. Bagge, M. Hjelm, C. Johansen, I. Huber and L. Grami, *Appl Environ Microb*, 2001, **67**, 2319-2325.
4. A. G. Shard and P. E. Tomlins, *Regen Med*, 2006, **1**, 789-800.
5. J. H. Hanemaaijer, T. Robbertsen, T. Vandenboomgaard and J. W. Gunnink, *J Membrane Sci*, 1989, **40**, 199-217.
6. E. Dickinson, *Food Hydrocolloids*, 1986, **1**, 3-23.
7. J. M. Nam, C. S. Thaxton and C. A. Mirkin, *Science*, 2003, **301**, 1884-1886.
8. S. R. Weinberger, T. S. Morris and M. Pawlak, *Pharmacogenomics*, 2000, **1**, 395-416.
9. E. Katz and I. Willner, *Angew Chem Int Ed Engl*, 2004, **43**, 6042-6108.
10. A. Hung, S. Mwenifumbo, M. Mager, J. J. Kuna, F. Stellacci, I. Yarovsky and M. M. Stevens, *J Am Chem Soc*, 2011, **133**, 1438-1450.
11. M. Lundqvist, I. Sethson and B.-H. Jonsson, *Langmuir*, 2004, **20**, 10639-10647.
12. P. Roach, D. Farrar and C. C. Perry, *J Am Chem Soc*, 2006, **128**, 3939-3945.
13. A. A. Vertegel, R. W. Siegel and J. S. Dordick, *Langmuir*, 2004, **20**, 6800-6807.
14. S. Song, Y. Qin, Y. He, Q. Huang, C. Fan and H. Y. Chen, *Chem Soc Rev*, 2010, **39**, 4234-4243.
15. J. N. Israelachvili, *Intermolecular and surface forces*, Academic press, 2011.
16. M. M. Elmahdy, C. Gutsche and F. Kremer, *J Phys Chem C*, 2010, **114**, 19452-19458.
17. J. N. Israelachvili and G. E. Adams, *Journal of the Chemical Society, Faraday Transactions 1: Physical Chemistry in Condensed Phases*, 1978, **74**, 975-1001.
18. D. Velegol, J. L. Anderson and S. Garoff, *Langmuir*, 1996, **12**, 4103-4110.
19. C. E. McNamee, M. Kappl, H. J. Butt, J. Ally, H. Shigenobu, Y. Iwafuji, K. Higashitani and K. Graf, *Soft Matter*, 2011, **7**, 10182-10192.
20. W. A. Ducker, T. J. Senden and R. M. Pashley, *Nature*, 1991, **353**, 239-241.
21. H. J. Butt, B. Cappella and M. Kappl, *Surf Sci Rep*, 2005, **59**, 1-152.
22. L. Meagher and H. J. Griesser, *Colloid Surface B*, 2002, **23**, 125-140.
23. J. J. Valle-Delgado, J. A. Molina-Bolivar, F. Galisteo-Gonzalez, M. J. Galvez-Ruiz, A. Feiler and M. Rutland, *Phys Chem Chem Phys*, 2004, **6**, 1482-1486.
24. J. J. Valle-Delgado, J. A. Molina-Bolivar, F. Galisteo-Gonzalez, M. J. Galvez-Ruiz, A. Feiler and M. W. Rutland, *Langmuir*, 2006, **22**, 5108-5114.
25. L. C. Xu and B. E. Logan, *Langmuir*, 2006, **22**, 4720-4727.
26. K. E. Bremmell, P. Kingshott, Z. Ademovic, B. Winther-Jensen and H. J. Griesser, *Langmuir*, 2006, **22**, 313-318.
27. M. A. Cole, N. H. Voelcker, H. Thissen, R. G. Horn and H. J. Griesser, *Soft Matter*, 2010, **6**, 2657-2667.
28. T. S. Tsapikouni, S. Allen and Y. F. Missirlis, *Biointerphases*, 2008, **3**, 1-8.
29. I. Larson, C. J. Drummond, D. Y. C. Chan and F. Grieser, *J Am Chem Soc*, 1993, **115**, 11885-11890.
30. S. W. Prescott, C. M. Fellows, R. F. Considine, C. J. Drummond and R. G. Gilbert, *Polymer*, 2002, **43**, 3191-3198.
31. E. Thormann, A. C. Simonsen, P. L. Hansen and O. G. Mouritsen, *Langmuir*, 2008, **24**, 7278-7284.
32. T. A. Camesano and B. E. Logan, *Environ Sci Technol*, 2000, **34**, 3354-3362.
33. K. E. Bremmell, A. Evans and C. A. Prestidge, *Colloid Surface B*, 2006, **50**, 43-48.
34. S. Iyer, R. M. Gaikwad, V. Subba-Rao, C. D. Woodworth and I. Sokolov, *Nat Nanotechnol*, 2009, **4**, 389-393.

35. I. Larson, C. J. Drummond, D. Y. C. Chan and F. Grieser, *The Journal of Physical Chemistry*, 1995, **99**, 2114-2118.
36. G. Toikka, R. A. Hayes and J. Ralston, *Langmuir*, 1996, **12**, 3783-3788.
37. M. Borkovec, I. Szilagyi, I. Popa, M. Finessi, P. Sinha, P. Maroni and G. Papastavrou, *Adv Colloid Interfac*, 2012, **179–182**, 85-98.
38. M. Finessi, P. Sinha, I. Szilagyi, I. Popa, P. Maroni and M. Borkovec, *J Phys Chem B*, 2011, **115**, 9098-9105.
39. G. Singh, S. Pillai, A. Arpanaei and P. Kingshott, *Adv Mater*, 2011, **23**, 1519-1523.
40. E. F. Osserman, R. E. Canfield and S. Beychok, *Lysozyme*, Academic press, 1974.
41. T. Peters and ScienceDirect, *All about albumin: biochemistry, genetics, and medical applications*, Academic Press San Diego, 1996.
42. J. P. Cleveland, S. Manne, D. Bocek and P. K. Hansma, *Rev Sci Instrum*, 1993, **64**, 403-405.
43. H. Ohshima, *J Colloid Interf Sci*, 1998, **198**, 42-52.
44. D. Mccormack, S. L. Carnie and D. Y. C. Chan, *J Colloid Interf Sci*, 1995, **169**, 177-196.
45. N. Denkov, O. Velev, P. Kralchevski, I. Ivanov, H. Yoshimura and K. Nagayama, *Langmuir*, 1992, **8**, 3183-3190.
46. G. Singh, S. Pillai, A. Arpanaei and P. Kingshott, *Soft Matter*, 2011, **7**, 3290-3294.
47. T. Arai and W. Norde, *Colloid Surface*, 1990, **51**, 1-15.
48. R. A. Hartvig, M. van de Weert, J. Ostergaard, L. Jorgensen and H. Jensen, *Langmuir*, 2011, **27**, 2634-2643.
49. J. L. Robeson and R. D. Tilton, *Langmuir*, 1996, **12**, 6104-6113.
50. M. Boström, D. R. M. Williams and B. W. Ninham, *Biophys J*, 2003, **85**, 686-694.
51. K. R. Babu and V. Bhakuni, *Eur J Biochem*, 1997, **245**, 781-789.
52. G. Damaschun, H. Damaschun, K. Gast and D. Zirwer, *J Mol Biol*, 1999, **291**, 715-725.
53. L.-C. Xu, V. Vadillo-Rodriguez and B. E. Logan, *Langmuir*, 2005, **21**, 7491-7500.
54. N. I. Abu-Lail and T. A. Camesano, *Biomacromolecules*, 2003, **4**, 1000-1012.
55. D. Stigter, D. O. V. Alonso and K. A. Dill, *P Natl Acad Sci USA*, 1991, **88**, 4176-4180.
56. H. L. Zhang, K. E. Bremmell and R. S. Smart, *J Biomed Mater Res A*, 2005, **74A**, 59-68.
57. P. M. Claesson, E. Blomberg, J. C. Froberg, T. Nylander and T. Arnebrant, *Adv Colloid Interfac*, 1995, **57**, 161-227.
58. T. J. Su, J. R. Lu, R. K. Thomas, Z. F. Cui and J. Penfold, *Langmuir*, 1998, **14**, 438-445.
59. J. B. Matthew and F. R. N. Gurd, *Method Enzymol*, 1986, **130**, 413-436.
60. B. W. Matthews, *Adv Protein Chem*, 1995, **46**, 249-278.
61. H. Wang, V. Singh and S. H. Behrens, *The Journal of Physical Chemistry Letters*, 2012, **3**, 2986-2990.
62. M. U. Hammer, T. H. Anderson, A. Chaimovich, M. Scott Shell and J. Israelachvili, *Faraday discussions*, 2010, **146**, 299-401.
63. F. Petit, R. Audebert and I. Iliopoulos, *Colloid Polym Sci*, 1995, **273**, 777-781.
64. D. E. Kuehner, J. Engmann, F. Fergg, M. Wernick, H. W. Blanch and J. M. Prausnitz, *J Phys Chem B*, 1999, **103**, 1368-1374.
65. L. Chun-Chih, N. Motta and M. John, *International Journal of Nanoscience*, 2008, **7**, 299-303.
66. I.M. Kempson, P. Chang, K. Bremmell, C.A. Prestidge, *Langmuir*, 2013, *29(50)*, 15573-15578.

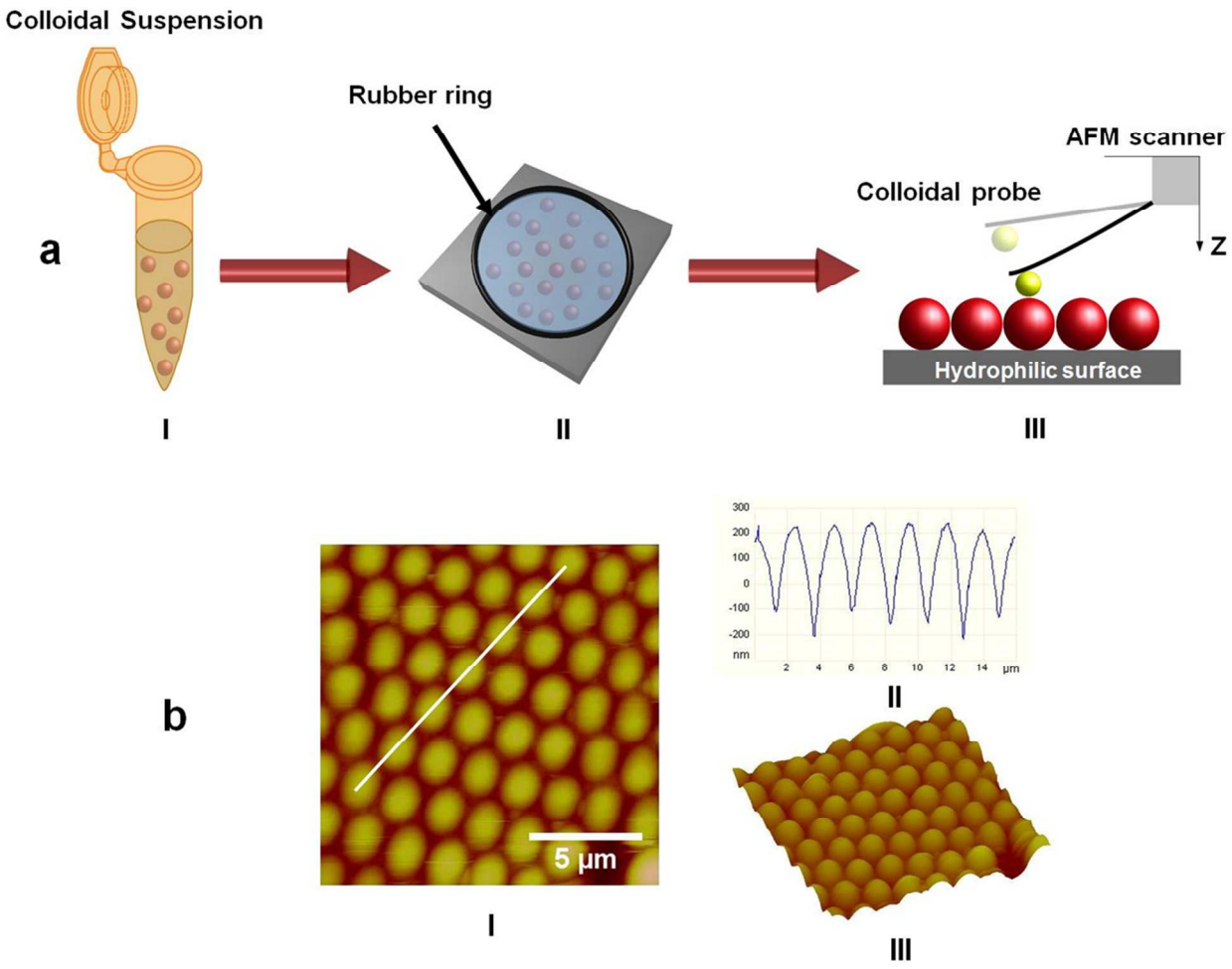

Fig.1 (a) Schematic illustration of the colloid probe AFM measurements, (I) prepared colloidal suspension, (II) drop casting of colloidal suspension onto a hydrophilic surface encircled by a rubber ring, (III) colloidal crystal formation after complete evaporation, and force measurements using colloid probe. (b) Contact mode AFM topographical representation of a 2 µm COOH-PS self-assembled colloidal crystal; (I) 2D view, (II) section analysis of image (I) showing center to center distance 2 µm, (III) 3D topography.

Cite this: DOI: 10.1039/c0xx00000x

www.rsc.org/xxxxxx

ARTICLE TYPE

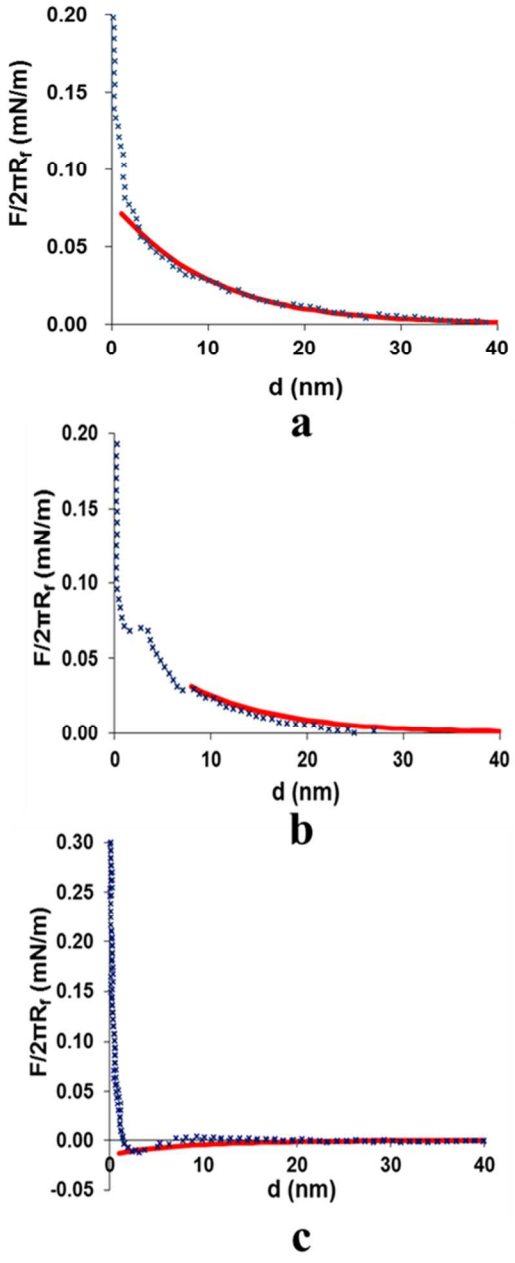

Fig.2 Normalized force ($F/2\pi R_f$) versus apparent separation (d) approach curves for the interaction between a PS colloid-probe and surface patterned with (a) 2 µm COOH-PS, (b) 2 µm silica and (c) 2 µm COOH-PS (PEI) particles. The force curves were measured in 1 mM NaCl solution (pH=7.4). The solid red line represents the theoretical fit using surface potential of probe, $\varphi_{probe\text{-}PS}$= -28.9 mV and particles (a) $\varphi_{2\mu m\text{-}PS}$= -19.8 mV, (b) $\varphi_{2\mu m\text{-}silica}$= -21.3 mV, (c) $\varphi_{2\mu m\text{-}PS(PEI)}$= +5 mV. The Debye length (κ^{-1}) determined from fit corresponds to the ionic strength of solution (9.6 nm for 1 mM NaCl).

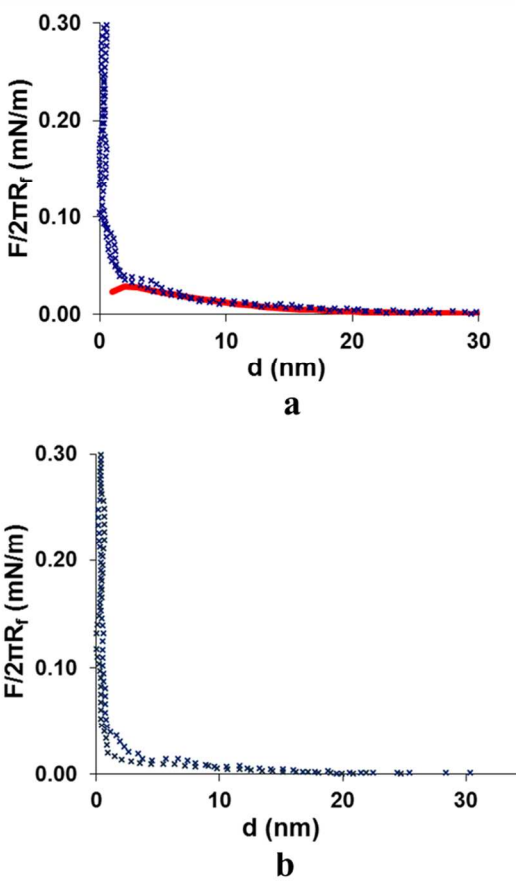

Fig.3 Normalized force versus apparent separation approach curves for the interaction between a PS colloid-probe and surface patterned with LZM modified (a) 2 µm COOH-PS, (b) 2 µm silica particles in 1 mM NaCl (pH=7.4). The solid red line represents the theoretical fit using surface potential (a) $\varphi_{probe\text{-}PS}$= -28.9 mV and $\varphi_{2\mu m\text{-}PS(LZM)}$= -4.7 mV. The Debye length (κ^{-1}) determined from fit corresponds to the ionic strength of solution (9.6 nm for 1 mM NaCl).

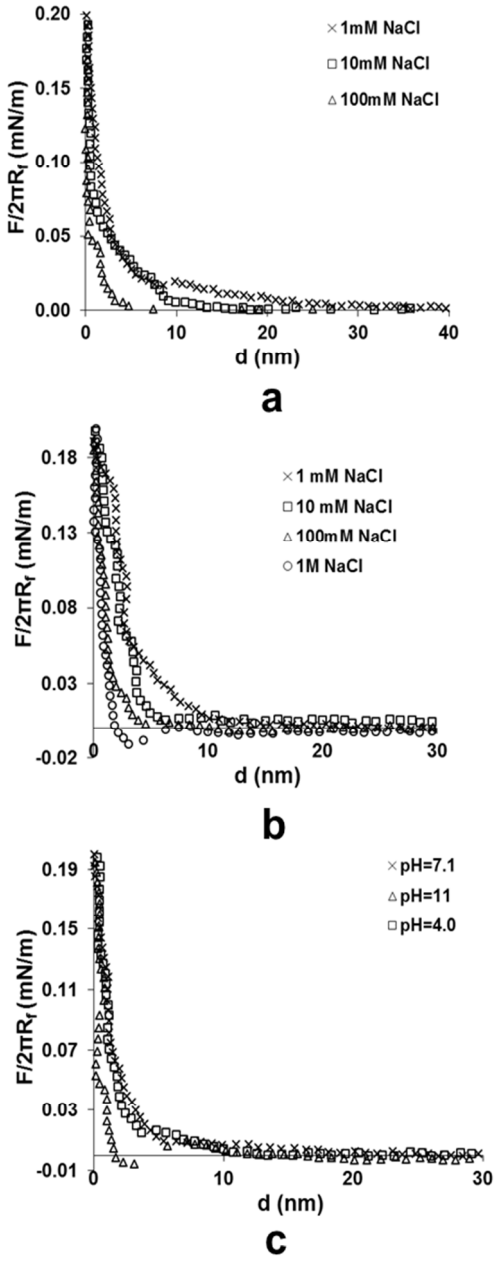

Fig.4 Normalized force versus apparent separation approach curves for the interaction between a colloid-probe and surface patterned with LZM modified (a) 2 μm COOH- PS particles in different NaCl concentration, and 2 μm silica particles in different (b) NaCl concentration, (c) pH values (1 mM NaCl).

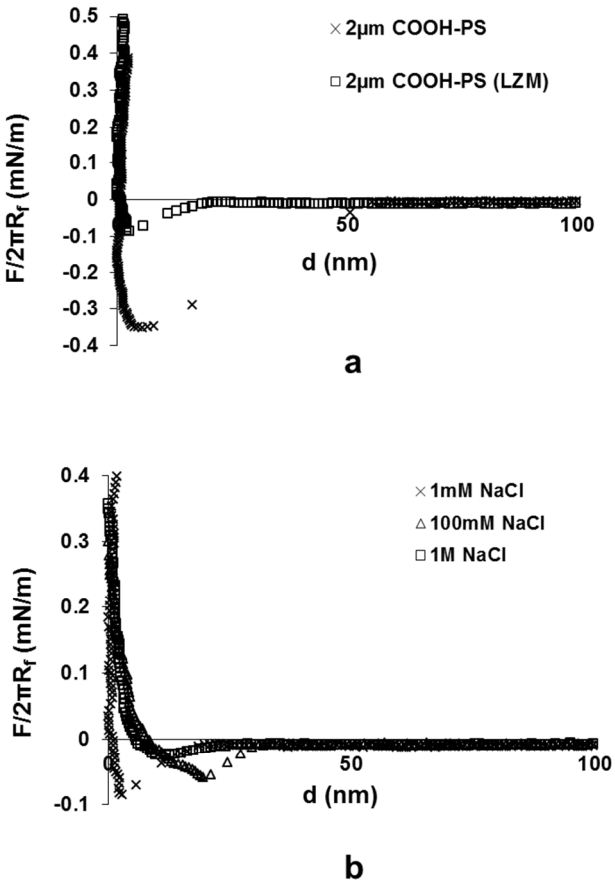

Fig.5 Normalized force versus apparent separation retraction curves show (a) forces of adhesion between a colloid-probe and surface patterned from with or without LZM modified 2 μm COOH-PS particles, and (b) adhesive forces between a probe and LZM modified 2 μm COOH-PS particle patterned surface in different NaCl concentration.

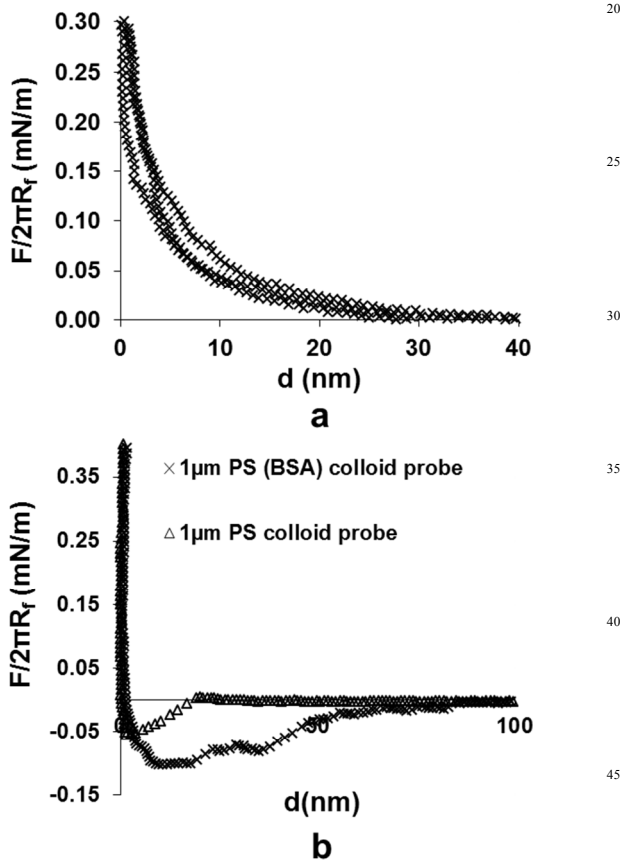

Fig.6 Normalized force versus apparent separation (a) approach curves collected for the interaction between a BSA modified colloid-probe and surface patterned with LZM coated 2 μm COOH-PS particles, and (b) retraction curves for the interaction between a probe with or without BSA modification and surface patterned with LZM coated 2 μm COOH-PS particles.

Particle type	1 mM NaCl (pH=7.4)	10 mM NaCl (pH=6.9)
2 μm COOH-PS	-19.8 mV	-8.9 mV
2 μm COOH-PS (PEI)	29.4 mV	7.3 mV
2 μm COOH-PS (LZM)	-4.7 mV	3.4 mV
2 μm silica	-21.3 mV	-10.8 mV
2 μm silica (LZM)	1.4 mV	3.3 mV
1 μm PS	-28.9 mV	-20.3 mV
1 μm PS (BSA)	-13.9	-5.3 mV

Table 2 Zeta potential measurements in different aqueous medium.

TOC